



**QUEEN'S
UNIVERSITY
BELFAST**

Cantilever steel post damaged by wind

Sha, W., & Malinov, S. (2014). Cantilever steel post damaged by wind. *Case Studies in Engineering Failure Analysis*, 2(2), 162–168. <https://doi.org/10.1016/j.csefa.2014.09.001>

Published in:
Case Studies in Engineering Failure Analysis

Document Version:
Publisher's PDF, also known as Version of record

Queen's University Belfast - Research Portal:
[Link to publication record in Queen's University Belfast Research Portal](#)

Publisher rights

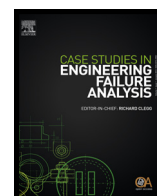
2014 The Authors. Published by Elsevier Ltd. Th
This is an open access article under the CC BY-NC-ND license (<http://creativecommons.org/licenses/by-nc-nd/3.0/>) which permits distribution and reproduction for non-commercial purposes, provided the author and source are cited.

General rights

Copyright for the publications made accessible via the Queen's University Belfast Research Portal is retained by the author(s) and / or other copyright owners and it is a condition of accessing these publications that users recognise and abide by the legal requirements associated with these rights.

Take down policy

The Research Portal is Queen's institutional repository that provides access to Queen's research output. Every effort has been made to ensure that content in the Research Portal does not infringe any person's rights, or applicable UK laws. If you discover content in the Research Portal that you believe breaches copyright or violates any law, please contact openaccess@qub.ac.uk.



Case report

Cantilever steel post damaged by wind

Wei Sha^{a,*}, Savko Malinov^b^a School of Planning, Architecture and Civil Engineering, Queen's University Belfast, Belfast BT7 1NN, UK^b School of Mechanical and Aerospace Engineering, Queen's University Belfast, Belfast BT7 1NN, UK

ARTICLE INFO

Article history:

Received 21 April 2014

Received in revised form 17 August 2014

Accepted 3 September 2014

Available online 16 September 2014

Keywords:

Structural steel

Cracks

Fracture

Metallurgical failure analysis

Surface layers

ABSTRACT

An analysis for the cause of fracture failure of a cantilever steel sign post damaged by wind has been carried out. An unusual cause of failure has been identified, which is the subject of this paper. Microscopy and microanalysis of the fracture surface showed that the failure was due to pre-existing cracks, from the fabrication of the post. This conclusion was reached after detecting and analysing a galvanised layer on the fracture surfaces.

© 2014 The Authors. Published by Elsevier Ltd. This is an open access article under the CC BY-NC-ND license (<http://creativecommons.org/licenses/by-nc-nd/3.0/>).

1. Introduction

Bushmills Primary School, in Northern Ireland, has two electronic patrol signs (towards 100 kg each) on cantilever posts which were erected in November 2010. Over a period of time, the posts had been under a continuous swaying movement or vibration, caused by wind. Gusts and storms on 20 November 2013 caused one post to sheer in two places and fall with a consequence of blowing off the housing door. The post was situated in an exposed position. Fig. 1 shows the damage to the post. As can be seen in the photos, it broke at both the top and bottom of the aperture, at opposite ends. The post had an outer diameter of 142 mm, and a wall thickness of 4 mm. Luckily, the post fell outwards but live cables were exposed. The Department for Regional Development in Northern Ireland (DRDNI) was concerned about other similar cantilever posts and the appropriate Traffic Officers were made aware of this incident. This incident was reported through the procedures as set out in the health and safety manual used by DRDNI.

Bushmills Primary School had not noticed any damage to the sign prior to the gusts. The School crossing patrol officer again had not noticed any damage and believed the sign was operational that morning. The sign was located next to Bushmills Outdoor Education Centre. Staff from that building confirmed that the sign was blown down in the wind and they had not noticed any previous damage. The sign was overlooked by a number of houses, and nobody witnessed any vandalism. The sign had a live cable running through it. If it was cut by vandals, the chances are that the culprit would be electroshocked or electrocuted.

The post was then salvaged by cutting the remainder of the way through and removing the stump. The breaks are fairly straight and clean. The subsequent cuts show the marks of the angle grinder. The initial concern of the Roads Service is that this may be a fatigue failure due to cyclic loading within the design range rather than tensile failure due to the post being

* Corresponding author. Tel.: +44 28 90974017; fax: +44 28 90974278.

E-mail address: w.sha@qub.ac.uk (W. Sha).

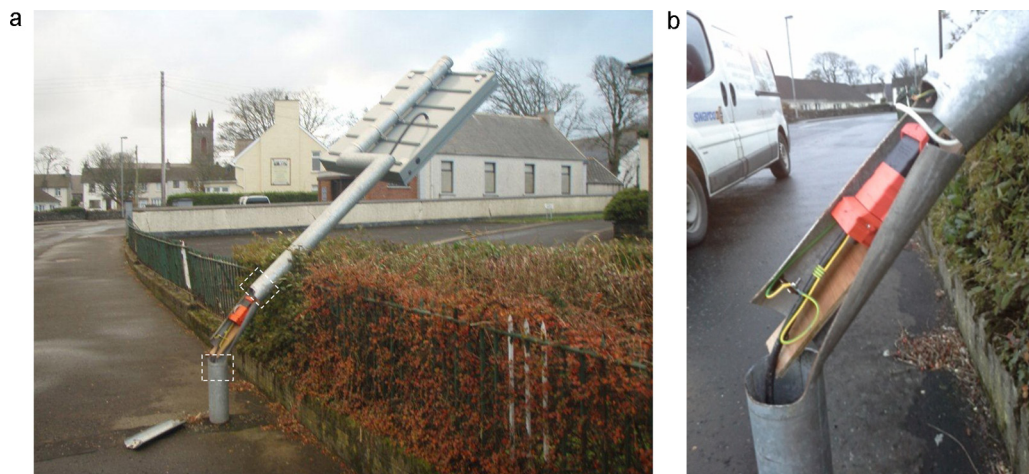


Fig. 1. Damaged cantilever post (optical macro-photographs of the fracture site courtesy of the Department for Regional Development in Northern Ireland). (a) The two dashed boxes show the bottom and top tubes, cut off after damaging, for analysis; (b) overview of the fracture sites.

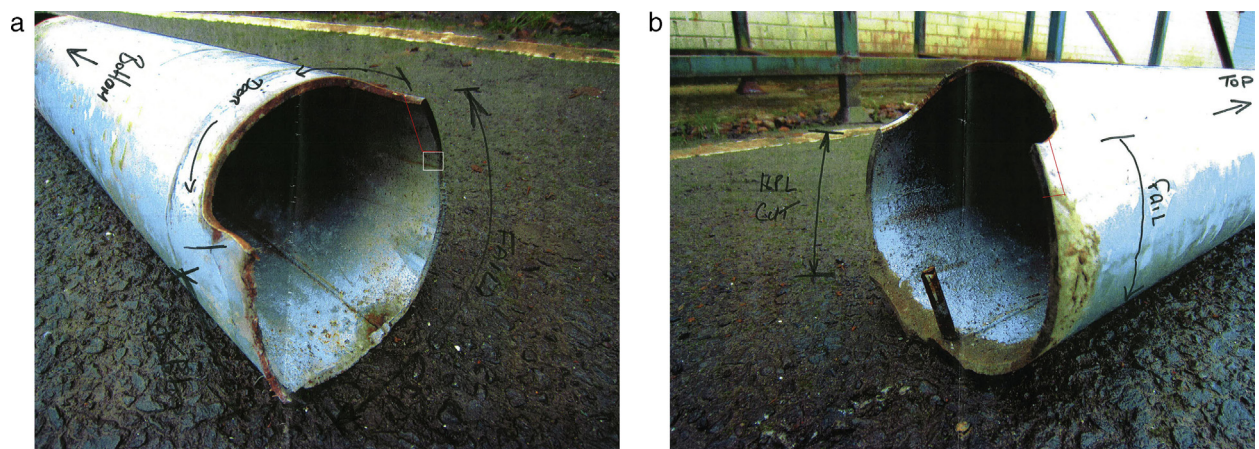


Fig. 2. Tubes cut from (a) the bottom and (b) the top parts of the damaged post (optical macro photographs of the regional fracture surfaces courtesy of the Department for Regional Development in Northern Ireland). The failed portion is labelled, as is the portion cut subsequently by angle grinder. The sampling locations are shown.

overstressed, and hence, that there may be other failures over time. These posts were designed with reference to the weakest point, the aperture, on the basis of a static wind load, with no consideration for dynamic loading. A rigid post with a heavy sign head would have reduced natural frequency, but in the right conditions, the amplitude of oscillation might increase and hence the induced stress. Notice a very much weaker and more flexible part near the base at the aperture.

Two sections were cut from the damaged post, shown in Fig. 2, and delivered to the first author to carry out a failure analysis, to identify the cause of failure.

2. Experimental

2.1. Tensile testing

Three tensile specimens were machined off the tube, in longitudinal direction, with the gauge length starting at 55 mm away from the fracture, to test the base tensile properties of the steel material. The gauge length of the tensile specimens is 90 mm, having the cross-section over the gauge length 3 mm × 10 mm. An Amsler tensile/compression testing machine was used, with a strain rate of approximately 10 mm/min.

2.2. Sampling and electron microscopy

Two fracture surface samples were cut, one from each tube provided, in the positions shown with red lines, in Fig. 2. These will be referred to as “bottom” (Fig. 2a) and “top” (Fig. 2b) fracture surfaces, according to their location relative to the door on

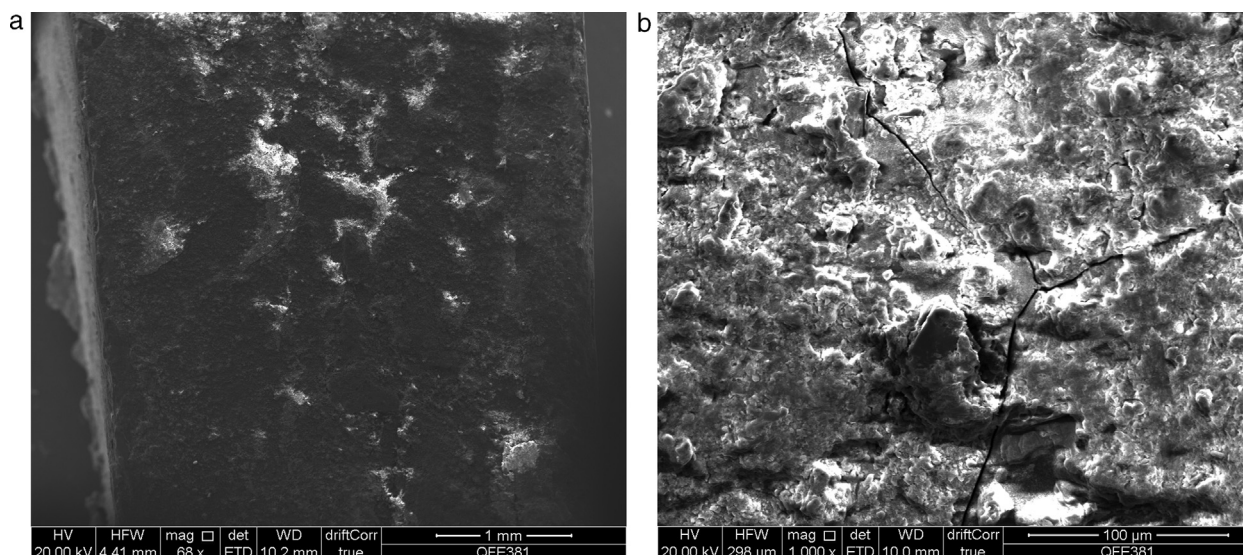


Fig. 3. Fracture surface from the bottom tube, at (a) low and (b) high magnifications as shown by the scale bar on bottom right of the images.

the post. Only the fracture surfaces on these two samples were examined. Other cut surfaces and the tube inside and outside walls, on these two samples, were not examined.

A further sample, shown with the white box on Fig. 2a, was cut, from the bottom tube. The longitudinal section, along the top line of the white box in Fig. 2a, i.e., to match the bottom red line, was mounted in resin especially suitable for scanning electron microscopy experiments, ground and polished. This sample will be referred to as the “section” sample.

A field-emission scanning electron microscope (FE-SEM, QUANTA FEG250) equipped with OXFORD X-Act as chemical composition analyser was used to study the surface morphology and composition. Energy dispersive X-ray (EDX) run by Aztec version 2.0 software was used for chemical composition analysis.

3. Results and discussion

3.1. Tensile properties

Tensile stress–strain curves are typical of mild steel. Averaging from the three tests, the yield stress is 472 ± 35 MPa and the tensile strength is 558 ± 8 MPa. The large standard deviation of the yield stress is due to the limited number of data points recorded during the tensile test, and thus the possibility of missing the true yield point among the resulting dataset. The average UTS/YS ratio is 1.19 ± 0.07 , from the three tests. The average elongation at UTS is $13 \pm 2\%$, and that at fracture is $17 \pm 4\%$. There is large plateau at UTS, lasting on average $3 \pm 2\%$ strain. The elongation at fracture value calculated from the stress–strain curves is the same as measured manually off the broken specimens. Necking was observed.

3.2. Fracture surfaces

The fracture surface does not look like that for typical steels [1]. See SEM images in Fig. 3. Two fracture tube faces show a same morphology, so only one is shown in Fig. 3.

Chemical analysis of this surface, Table 1, showed that the surface composition is mainly ZnO, and not iron or steel. The composition shown in Table 1 was averaged from six analyses in six different locations, of the two fracture surface specimens, one from top and one from bottom parts of the broken post. This explains why the fracture surface appearance does not look like steel fracture surface. The actual error on the analysed result of O may be larger than that shown in Table 1, as EDS is not good at analysing light elements.

The finding was that the surface composition is mainly ZnO. However, the EDS only analyses the composition of a few micrometres from the surface. It does not penetrate deep into the surface, as electrons, even after acceleration using a 20 kV voltage drop, cannot travel far in solid.

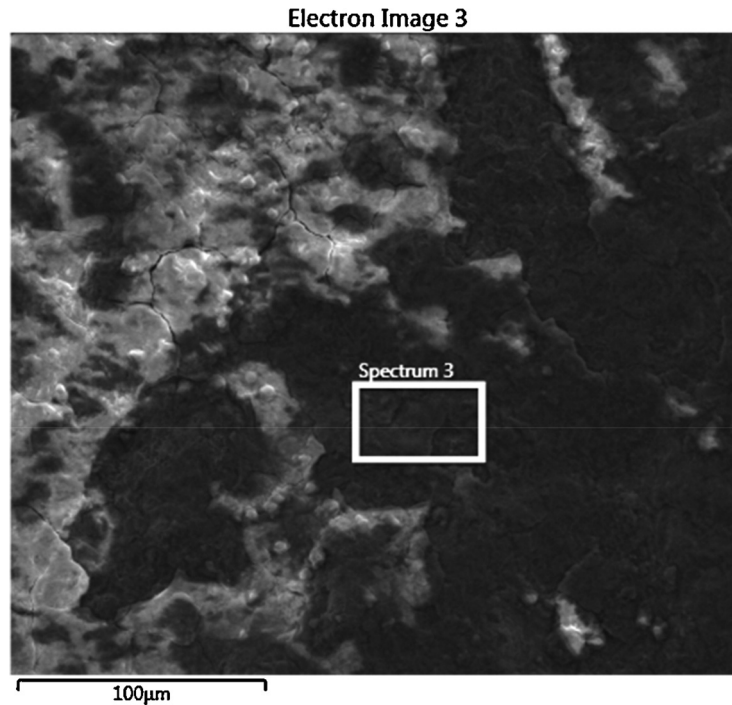
So, the cracks shown in Fig. 3b are cracks of ZnO, and are not necessarily cracks of steel, underneath the surface ZnO layer.

So, it was not possible to examine the actual steel fracture surface, but this would turn out to be unnecessary, as far as the cause of fracture is concerned, as will be seen from later discussions. It was hoped to examine the steel fracture surface in order to tell whether the fracture is brittle, ductile, creep or fatigue, but as we are looking at ZnO layers on the fracture surface, we do not see the actual steel.

Table 1

Chemical composition (wt.%) of the fracture surface analysed by energy dispersive X-ray spectrometry.

Location	Zn	O	Fe	Si	Na	Al	Mg	Ca	Mn
Fracture surfaces	41.4 ± 5.3	37.7 ± 3.9	6.1 ± 1.7	5.7 ± 1.3	3.4 ± 1.8	2.9 ± 0.9	1.5 ± 0.4	1.1 ± 0.3	0
Spectrum 3 in Fig. 4	17.4 ± 0.5	33.1 ± 0.5	44.5 ± 0.5	0	2.3 ± 0.5	0	1.9 ± 0.2	0.3 ± 0.1	0.5 ± 0.1
Spectrum 6 in Fig. 7	35.0 ± 0.5	29.6 ± 0.4	28.0 ± 0.4	0.9 ± 0.1	4.3 ± 0.5	0	1.4 ± 0.1	0.3 ± 0.1	0.5 ± 0.1

**Fig. 4.** Fracture surface from top tube, showing the local absence of the ZnO layer.

Some parts of the ZnO layer were broken or torn off, revealing the steel surface, partially corroded and darker upon imaging (Fig. 4). Chemical analysis showed that the exposed darker parts were mainly oxidised steel. For example, analysis of the area labelled Spectrum 3 in Fig. 4 gave a composition shown in Table 1. Note again that all chemical analyses given in the paper only show composition of the top few micrometres of the surface that we are looking at. So, the analysis of Spectrum 3 in Table 1 is likely result of a mixture of the residual zinc coating (very thin so the electrons could penetrate through) and the real steel underneath. Mn is from the bulk mild steel. Some dotted rust was seen by naked eye on this fracture surface, presumably due to the steel exposing after parts of the zinc layer were torn or broken off.

Fig. 5 shows vividly the tearing of the zinc layer, still attached to the rest on one side. The steel exposed in the hole would readily corrode, and may be one of the dotted rust spots (about 0.3 mm in size, in this case), when looking at this specimen with the naked eye.

However, other parts of the zinc coating, on the fracture surface, were fine (Fig. 3a).

Summarising, the fractographic images show fracture surfaces covered with zinc, so they were not the direct fracture surfaces of the tube steel. As will be explained later, there would be no need to try to clean the fracture surfaces to rid the zinc of it. The finding of the zinc on the fracture surface in itself would identify the cause of failure.

3.3. Longitudinal section

This sample has proved valuable. Fig. 6 is explained below.

The top of Fig. 6a is the fracture surface, seen from longitudinal section. Ignore the small burr pieces above it, separate from the main specimen. They were result of longitudinal sectioning (cutting). The width is the thickness of the tube. Mounting resin is shown outside (left, top, right) the brighter specimen. The boxed area is magnified in the next picture, Fig. 6b.

In Fig. 6b, mounting resin is shown outside (left) the brighter specimen. Ignore the long and straight scratch lines in Fig. 6, caused during grinding and polishing of the specimen.

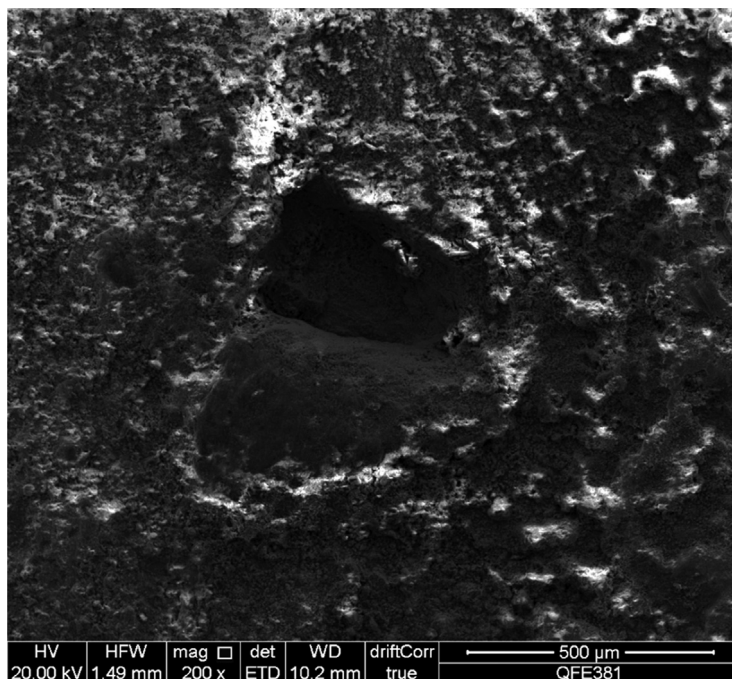


Fig. 5. Tearing of the zinc layer.

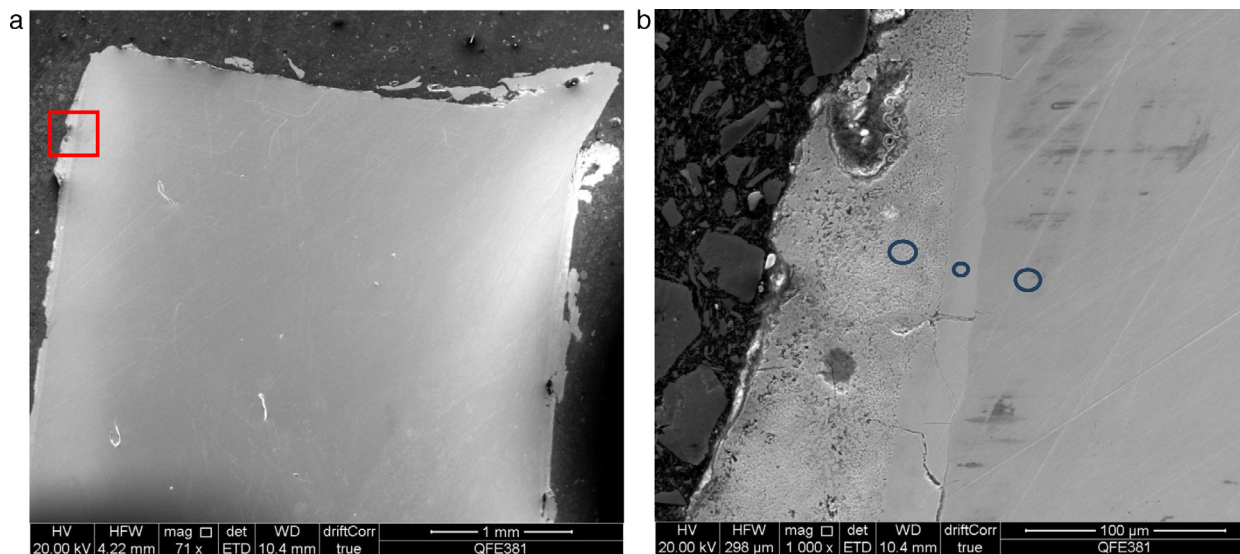


Fig. 6. Scanning electron micrographs of the longitudinal section. (a) Low magnification picture; (b) high magnification showing the zinc galvanised layers and areas for chemical analyses.

3.3.1. Galvanised tube wall

Fig. 6b shows galvanised inside tube wall. The outside tube wall, on the right hand side surface of Fig. 6a, would have similar features, but was not imaged. This figure shows galvanised zinc layers beautifully. The composition of the area marked by the left oval in Fig. 6b is 92%Zn, 6%Fe, 2%O. The composition of the area marked by the middle oval is 90%Zn, 8%Fe, 1%O. The composition of the area marked by the right oval is 99.5%Fe, 0.5%Mn, typical of mild steel. Electron microprobe cannot detect carbon when it is, say, 0.2%, as in mild steel. There are only three elements detected in the galvanised layers.

Such layered structure of galvanised zinc is typical. Note that this was from tube inside wall, and so should not be relevant to the fracture, but it serves as an identification of galvanised layer, and a calibration of the analysis.

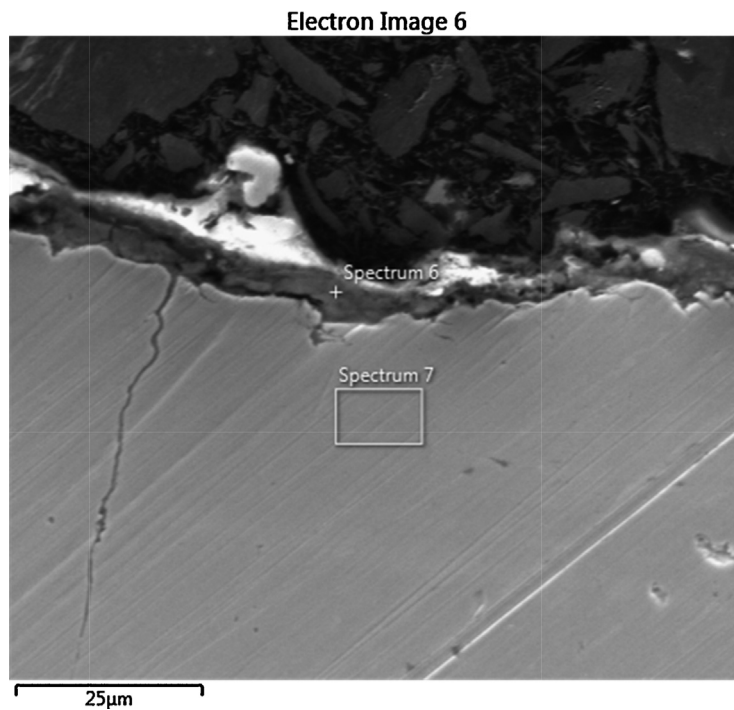


Fig. 7. Scanning electron micrograph of the longitudinal section, showing the cross-section of the fracture surface. Mounting resin is shown outside (top) the brighter specimen.

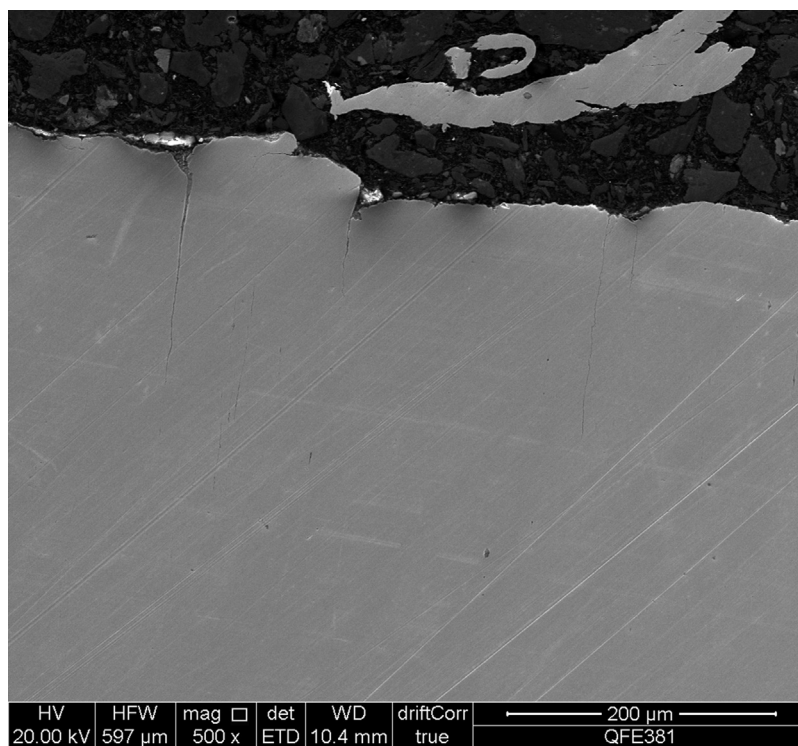


Fig. 8. Scanning electron micrograph of the longitudinal section. Mounting resin is shown outside (top) the brighter specimen. Ignore the small burr pieces at the top, separate from the main specimen. They were produced during longitudinal sectioning (cutting).

3.3.2. Longitudinal section of the fracture surface

The zinc found on the fracture surface in Section 3.2 was verified when examining the longitudinal section of the fracture surface, i.e., the top surface shown in Fig. 6a, now magnified in Fig. 7. The result of the chemical analysis of the location marked “Spectrum 6” is included in Table 1. The analysis of the area marked “Spectrum 7” gave the composition of steel, Fe- $(1.2 \pm 0.3)\%$ Mn.

There are long cracks parallel to the tube walls, shown in Figs. 7 and 8. It is inevitable for tubes to have anisotropic features, in longitudinal and cross-sectional directions, due to rolling defects along the rolling, i.e., longitudinal, direction. The cracks shown in Figs. 7 and 8 reflect these defects in the rolling direction, i.e., the axial direction of the tube. However, it is also clear that the cracks are only at near fracture surface areas, so they must have been formed at the surface and propagated to under the surface, to considerable depth. It is like delamination, but initiating only at the fracture surface.

4. Analysis of cause of failure

The zinc layer on the fracture surfaces would suggest that the fracture surfaces, both from top and bottom tubes, were not fresh fracture, as they did not show fresh steel (or even the corroded steel, corroded after fracture), but were previously galvanised surfaces. These could only be cracks formed when the door on the tube was cut, before galvanising. Obviously, such cracks would have been the weakest points of the tube, and so the tube broke along them.

Also, the fact that the failure planes were so straight, shown in Fig. 2, would point to the previously existing surfaces or cracks. Galvanised zinc colour is even visible on the fractured surface in Fig. 2.

An even further proof of the pre-existing cracks is that the KPL cut surfaces, shown in Fig. 2, are much more heavily corroded, compared to the fracture surfaces, as the latter has zinc “protection” on them. In Fig. 2, the parts labelled “FAIL” is clean and straight, compared to the rusted and rough “KPL” side.

It is not clear whether the delamination at near fracture surface formed long before the fracture (which led to the fracture when a significant number of delamination formed), or during the fracture (which was the result of the fracture). Either way, such delamination shows a weakness of the steel tube, parallel to the tube walls, but this is normal for thin, rolled steel.

Other elements found on the fracture surfaces (i.e., the pre-existing cracks) may be residual elements from the galvanising process, or accumulated over the years when the post was in service.

The tensile properties of the steel would not be the same as measured and given in Section 3.1, in the parts through the cracks of previously separated, and then galvanised surfaces.

5. Concluding remarks

In conclusion, the fracture failure was not due to weak or defected bulk steel (though delamination was noted, Section 3.3.2). Crack initiation did not happen in service, but during fabrication of the structure. Fracture was along a previously existing surface or interface, jointed together when the tubes were galvanised. During galvanising, these pre-existing cracks were filled with zinc, as found by the microscopy and microanalysis work. The cracks, unintentionally zinc filled, were of course much weaker than the parent steel. No tube would be able to survive such large cracks, albeit filled with zinc. The failure analysis was thus not about identifying bulk steel failure, because we did not have the continuous bulk steel in the tube, where the final failure happened.

Because the finding of these cracks identified the cause of the failure, it was not relevant or necessary to investigate fracture surface of steel, viz. the fracture surface of these pre-existing cracks. The existence of them was the cause of failure. This investigation thus was not a usual metal failure analysis, which tends to be around discussing mechanisms of failure such as brittle and much localized fracture, potential embrittlement caused by galvanisation, ductile rupture, fatigue including low cycle fatigue that could have been induced by corrosion pits so enhancing low cycle fatigue damaging.

The investigation performed has defined the mechanism of failure, by identification of fracture surface appearance, with possible hypothesis on root cause of the failure. Assumptions were made on the mechanism of failure on the basis of observations and proofs by quantitative analysis. However, the fractography in this work was different from that in the usual metal failure analysis. The key-point is in starting from assumptions to point out a hypothesis for failure cause and then verifying consistency of hypothesis. It is usually insufficient to claim one failure mode/mechanism as possible because other appears on opinion less probable, but the findings from this work was as conclusive as it could be on balance.

Acknowledgements

The authors would like to thank Colin Harris, Alan Keys, Deidre Mackle, and John McRobert, all of the Department for Regional Development in Northern Ireland, and Mr. Gault of Bushmills Primary School for providing the background information of the case study. John McRobert and Dr. Barry Rankin are also acknowledged for their contribution to discussion.

Reference

- [1] Sha W. *Steels: from materials science to structural engineering*. London: Springer; 2013.